2.17
Impregnation and Consolidation Phenomena

A. M. SASTRY
University of Michigan, Ann Arbor, MI, USA

2.17.1 INTRODUCTION

Process modeling of composite materials has rapidly advanced in the last 30 years, primarily due to the relatively recent ability to efficiently perform coupled fluid/reaction/solidification modeling. Impregnation describes the flow of resin into fiber tows. Consolidation describes the seamless compaction of laminae through interply flow of resin. Both are required in processing. Tailoring of process cycles to achieve adequate degree of cure (thermosets) or degree of crystallinity (thermoplastics) is also required. These steps enable materials selection for manufacturing characteristics, with simultaneous meaningful, real-time, process monitoring and control. Poor impregnation of composite materials results in unacceptably high void content, resin-rich areas, or other microstructural defects. Poor consolidation of composites results in similarly unacceptable mechanical properties, with the additional loss of control of matrix properties if curing of resins is not well-controlled with accurate models. This chapter discusses the underlying concepts of models for impregnation and consolidation phenomena.

2.17.2 PROCESSES AND KEY PHENOMENA

We concentrate on the manufacture of laminated composites processed by autoclave and compression molding; many of the concepts (including modeling of percolation-type fluid penetration problems) incorporate commonly used techniques for molded materials (see Chapters 2.20 and 2.22, this volume). A typical processing cycle for a laminated composite is shown schematically in Figure 1. The term "prepreg" refers to a preimpregnated lamina comprised of aligned fibers embedded in an uncured or partially cured resin. Use of such materials originated with a product called "scotchply," produced in the 1950s by Minnesota Mining and Manufacturing, Scotchply was composed

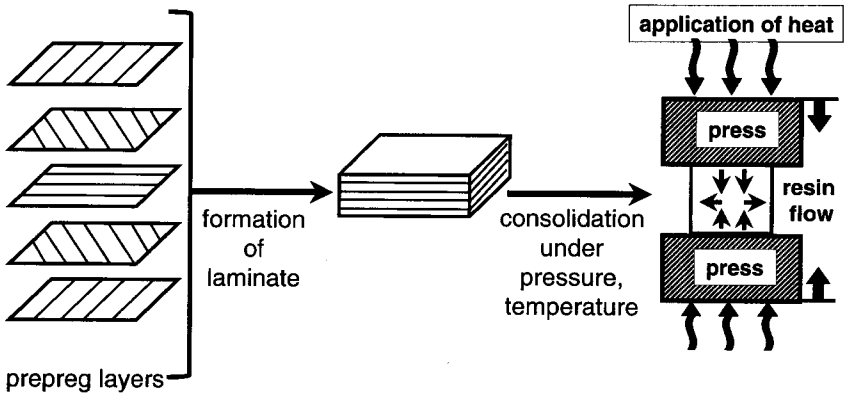

Figure 1 Basic processing of a laminated composite.

Table 1 General comparison of thermoset and thermoplastic composite processing.

Thermoplastic processing	*Thermoset laminate processing*
High viscosity at processing temperature	Lower viscosity at processing temperature
Shear thinning, extensional, viscoelastic flow	Primarily Newtonian flow
Significant effect of matrix shear on fibers	Primary flow mechanism: percolation
Short cycle times	longer cycle based on cure kinetics

of fibers embedded in a thermosetting resin (Halpin *et al.*, 1983). The majority of composite materials still feature such a thermosetting matrix or resin, although the use of thermoplastics has been widely viewed as the more promising technology due to the high processing rate, coupled with the possibility of simultaneous improvement in toughness and environmental resistance (e.g., Cogswell, 1992). Processing and consolidation of thermoplastic composite materials similarly requires careful consideration of changes in matrix viscosity over the cycle, but the crystallinity, rather than the degree of cure, is tracked, incorporating analysis of heat transfer in the mold or autoclave.

During thermoset processing, pressurization forces resin flow through the reinforcement, filling voids. Application of heat results in matrix cure. In thermoplastic processing, the molecular weight and degree of crystallinity are controlled. The process objective is a physical, rather than chemical, change in the matrix, unlike thermosetting cure, though cross-linking is a sometimes unintentional by-product of degradation of the matrix. Table 1 gives a general comparison of the two types of polymer processes. The key differences stem from two factors: the need to align process cycles with resin cure kinetics in the case of thermosets, and the need to manage impregnation with relatively larger processing viscosities encountered with thermoplastics.

Generally, process models for impregnation and consolidation of thermosets can be divided into three distinct but interdependent components, as shown in Figure 2. These divisions are similar for thermoplastics, except that physical, rather than kinetic, changes are tracked. In the first element, the curing of polymeric resins, we discuss the change in the resin response as it affects fluid constitutive response. Analysis of heat transfer is required to track resin cure kinetics, but a detailed discussion of heat transfer modeling is not given here. Some attention is paid to the effect of heat transfer in the resin, namely the influence of reaction on flow behavior. The second element, analysis of compaction of fibrous beds, involves modeling of fiber deformation in the presence of the surrounding fluid, which may impart significant shear stresses to the fibers. The third element, analysis of resin flow, comprises selection of an appropriate rheological model and application of the conservation equations to locate the flow path during processing.

The procedural elements in analysis of fluid flow are linked by material properties and geometry. Pressurization of a composite during processing, either by autoclave pressure on a vacuum-bagged material or via direct compression of a composite in a press, results in flow of resin through fiber reinforcement. The strategic application of temperature and pressure in a process cycle relies upon accurate

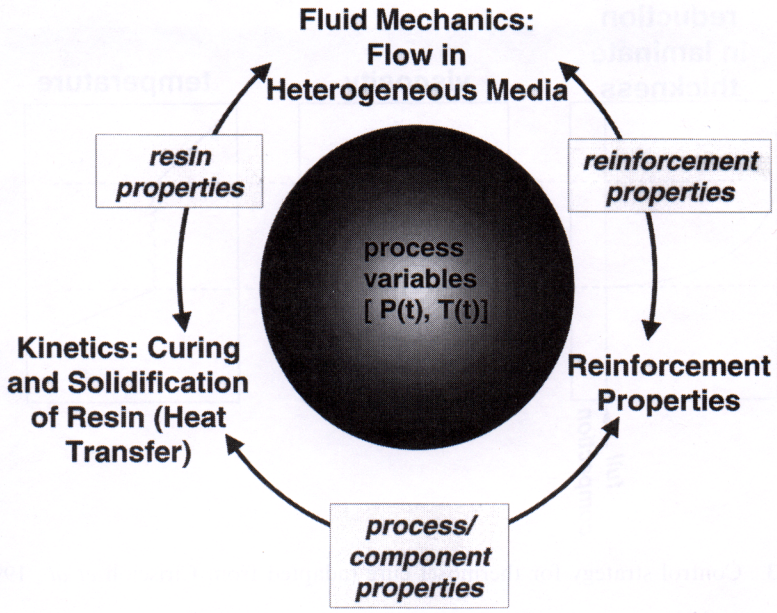

Figure 2 Three types of interdependent modeling inherent in impregnation and consolidation modeling of thermoset-matrix composites.

models for resin penetration of the reinforcement, alteration of the reinforcement microstructure due to compression, and changes in the resin properties.

2.17.3 THERMOSETTING RESINS: IMPORTANCE OF KINETICS, CURE, AND VISCOSITY

At a sufficiently high temperature in thermoset processing, reaction "ignition" occurs, and the resultant cross-linking causes a rapid increase in viscosity (see Chapter 2.19, this volume). During cure, reacting branched polymer molecules, spurred by a catalyzing agent, become irreversibly cross-linked with respect to temperature change below the decomposition temperature (Rodriguez, 1984). Neither cure nor viscosity can presently be directly measured during thermoset processing (Ciriscioli *et al.*, 1989, 1991). Ionic conductivity, however, can be measured and correlated with viscosity. Similarly, modified ionic conductivity can be measured and correlated with the degree of cure. Understanding the basic kinetic and rheological behavior allows tuning of processes to guarantee adequate resin flow in compacting laminae and proper temperature distribution for cure, while minimizing process cycles. Figure 3, adapted from Ciriscioli *et al.* (1991), illustrates an optimal strategy. This approach has achieved excellent results in thermoset process optimization (Ciriscioli and Springer 1992) with incorporation of real-time process control.

Successful control thermoset processing highlights the importance of the characterization of kinetics and rheology in materials and process design. Such analyses rely on accurate, generally semiempirical models. Experimental techniques to generate empirical parameters exist for characterizing resin cure behavior for both isothermal and nonisothermal conditions. While differential scanning calorimetry (DSC) and other methods accurately characterize certain parameters (e.g., the heat of reaction), others, such as contributions to the reaction rate from individual chemical reactions, cannot be determined with DSC alone. Thus, some simplification of kinetic models is generally required. Three key interdependent parameters are important in characterizing cure for process design: the heat of reaction, the degree of cure, and the resin viscosity. Most useful process models employ semiempirical relations to describe their interaction (e.g., Loos and Springer, 1983).

A brief example follows. The temperature dependence of a polymerization reaction rate constant can be expressed by the Arrhenius relation as

$$\kappa = \nu \exp\left(\frac{-E}{RT}\right) \tag{1}$$

where κ = reaction rate constant, ν = fitted constant, E = activation energy, T = temperature (absolute), and R = gas constant.

The approach taken in modeling kinetics in early classic work employed pseudo first-order

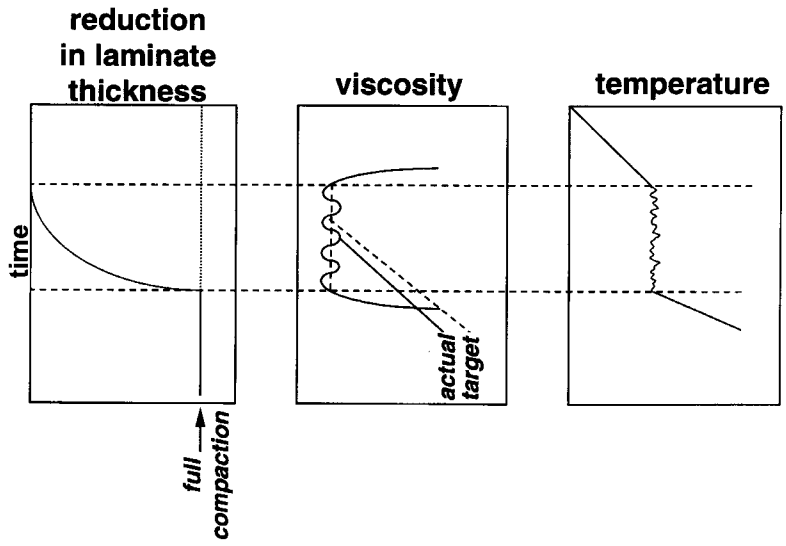

Figure 3 Control strategy for thermoset cure (adapted from Ciriscioli *et al.*, 1991).

kinetics. A pseudo first-order model is based on a single polymerization reaction

$$A \rightarrow P \tag{2}$$

wherein the reaction rate for species A may be written

$$\frac{dA}{dt} = rA = -\kappa A \tag{3}$$

where κ is the reaction rate constant per mole of species A reacted. For the Narmco 5208 system of Figure 4, the cure was shown (Halpin *et al.*, 1983) to follow a pseudo first-order reaction for epoxy-based systems. Polymer properties were determined via fitting of the kinetic model to experimental results using dynamic scanning calorimetry. Though two reactions occur in this system, one, the opening of an epoxide ring, has a significantly higher rate constant than the other, etherification of the epoxide and hydroxyl groups. Thus, the pseudo first-order model was based on the rate-limiting etherification step

$$-\frac{dA}{dt} = \kappa(T)[A] \tag{4}$$

where $[A]$ = concentration of epoxide groups and κ = apparent reaction rate and

$$p = 1 - e^{-\kappa(T)t} \tag{5}$$

where p = extent of reaction of epoxide groups, with the rate constant at temperature T given by

$$\kappa(T) = \alpha_k \kappa(T_o) \tag{6}$$

where

$$\ln \alpha_k = \frac{E}{R}\left(\frac{1}{T_o} - \frac{1}{T}\right) \tag{7}$$

DSC is the most widely used among experimental techniques for determination of reaction rate (e.g., Prime, 1973; Sourour and Kamal, 1976; Lee *et al.*, 1982; Loos and Springer, 1982; Halpin *et al.*, 1983). The approach involves heating of an uncured resin, followed by measurement of the heat evolved as it reacts. Both isothermal and nonisothermal conditions can be investigated using DSC. DSC is described in ASTM D 4473-95a (ASTM, 1995); in practice, it is frequently coupled with FTIR (Fourier transform infrared), GPC (gel permeation chromatography), IR or near-IR spectroscopy, and physical measurement of mechanical properties via viscometry or TMA (thermomechanical analysis).

Because DSC gives heat of reaction directly, degree of cure α may be defined conveniently as the heat evolved at a given time divided by the total heat of reaction, though definitions based on harder-to-measure properties such as molecular weight are possible. Total heat of reaction can be determined (e.g., Loos and Springer, 1983/1982) via

$$H_R = \int_0^{t_f} \left[\frac{dQ}{dt}\right] dt \tag{8}$$

where t_f is the amount of time required for completion of reaction. The cumulative amount of heat released at time t is given by

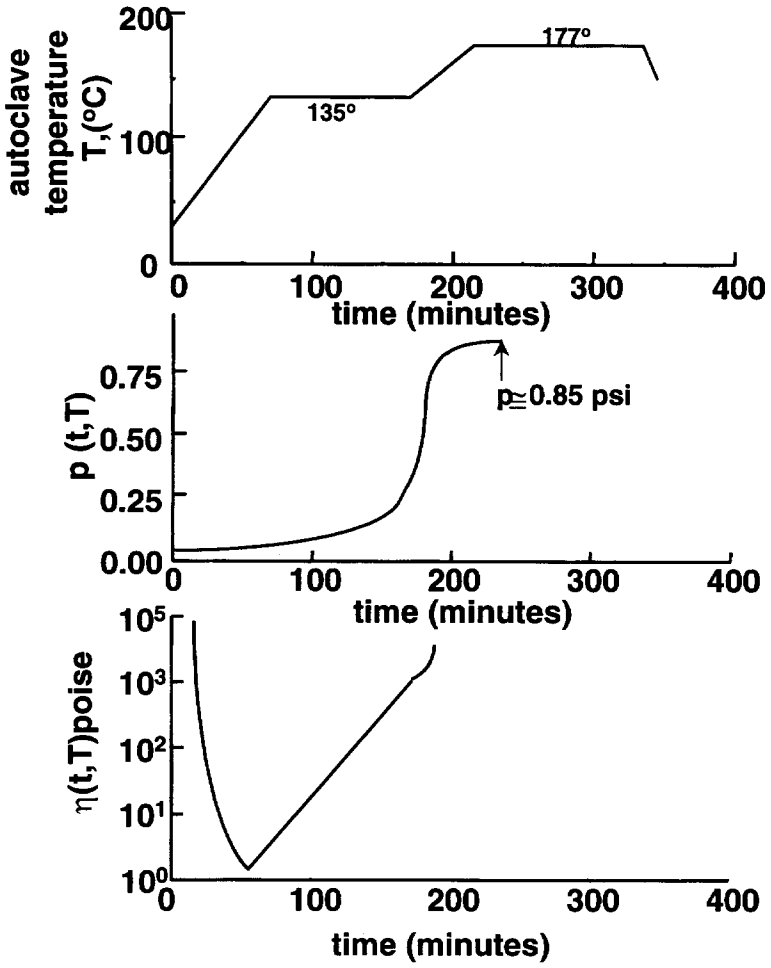

Figure 4 Sample cure cycle of Narmco 5208 system composite (adapted from Halpin *et al.*, 1983).

$$H_R = \int_0^t \left[\frac{dQ}{dt}\right] dt \tag{9}$$

whereupon degree of cure can be calculated as the ratio

$$\alpha = \frac{H}{H_R} \tag{10}$$

A relation for rate of cure $d\alpha/dt$ can be written as an Arrhenius relation; integration gives degree of cure as a function of time. Correlation of degree of cure with viscosity can be made via semiempirical models as that developed for Hercules 3501-6 resin (*ibid.*) by first developing assuming a form of relation for viscosity and degree of cure, as

$$\mu = \mu_\infty \exp\left(\frac{E}{RT} + B\alpha\right) \tag{11}$$

where μ_∞ and B are constants, and E is the activation energy for viscosity.

Kinetic models involving multiple reactions can also be derived (e.g., Kardos, 1997). Multiple reactions have also been more recently examined in epoxy systems (e.g., Chabert *et al.*, 1995; Lachenal *et al.*, 1997). For the widely used TGDDM–DDS (tetraglycidyl-4,4′-diaminodiphenylmethane 4,4′-diaminodiphenylsulfone) resin system, for example, improved determination of individual reaction enthalpies and reaction rates (using near-IR spectroscopy with DSC) allows some mapping of the concentration profiles of different groups formed over the whole range of cure (de Bakker *et al.*, 1993). Other recent work has produced more specialized mappings for viscosity, including parameters such as initial degree of cure (e.g., Theriault *et al.*, 1999).

As improvements in fundamental polymers experimentation and process control are achieved, it is likely that greater real-time control of process (coupled with extensive understanding of kinetic and rheological changes with process variables) will supplant empiricism in thermoset processing. Correlation of all of

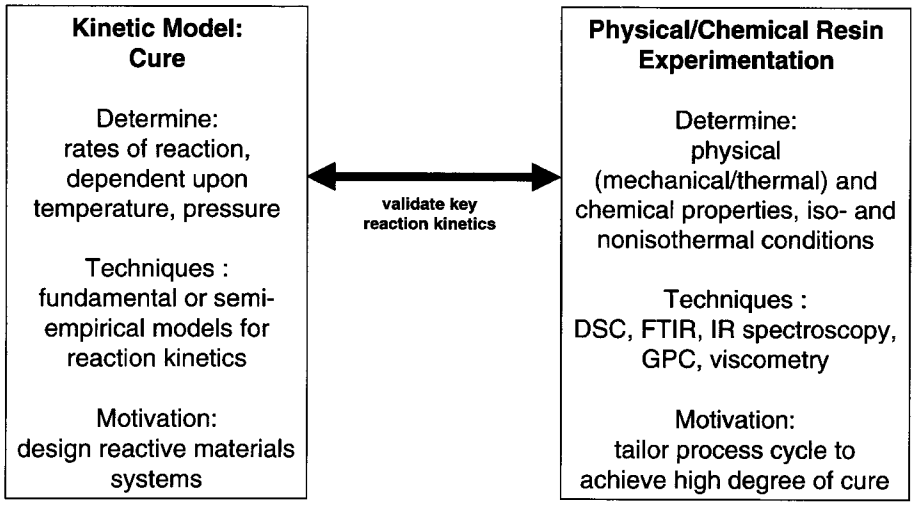

Figure 5 Summary of kinetic modeling and experimentation to determine physical resin properties for thermoset-matrix composites.

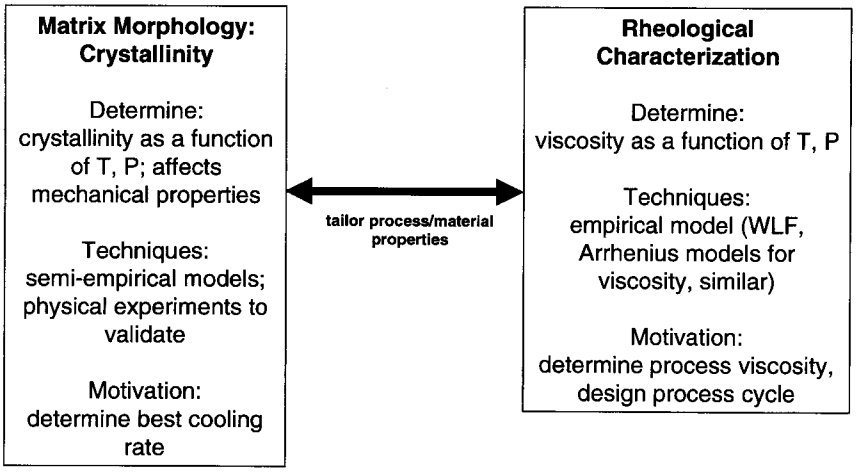

Figure 6 Summary of morphological and rheological modeling for thermoplastic-matrix composites.

these properties are summarized for thermosets in Figure 5.

2.17.4 THERMOPLASTIC MATRICES: PHYSICAL PROPERTIES

Unlike thermosetting resins, thermoplastic matrices do not generally form chemical cross-links, making them reprocessable (see Chapter 2.25, this volume). In this class of materials, morphology and rheology are be used to design process and material (Figure 6). Because these materials exhibit higher process viscosities than most thermosetting resins, consideration of impregnation and deformation of fiber reinforcement cannot be decoupled (e.g., Jones and Oakley, 1990). Instead, process models for thermoplastics must not only address physical properties of the resin, such as crystallinity of the final resin upon cooling, but also the deformation mechanics of the reinforcement (see Section 2.17.5). Bonding of layers, or autohesion, during which segments of long polymer chains migrate across thermoplastic lamina interfaces, is critical to assure good interfacial properties. Movement of polymer in the fibers was modeled by de Gennes (1971), who proposed the now classic "reptation" model for molecular movement, with polymer molecules moving in snakelike fashion inside of a strongly cross-linked gel.

Degree of autohesion has been defined (Dara and Loos, 1985; Lee and Springer, 1987) as

$$D_{au} = \frac{S}{S_\infty} \tag{12}$$

where S = bond strength at time t and S_∞ = ultimate bond strength (bond strength as $t \to \infty$).

Degree of autohesion is generally assumed to follow the relation (per Wool and Connor, 1981; Wool, 1982)

$$D_{au} = \chi t_a^{1/4} \tag{13}$$

and

$$\chi = \chi_o \exp(-E/RT) \tag{14}$$

where χ (Arrhenius-type) temperature-dependent constant, χ_0 = fitted constant, and E and R are the activation energy and the universal gas constant. A method for calculation for time to completion of bonding using a contact model, relating degree of contact with geometric and material parameters for the laminate, was developed by Lee and Springer (1987). Another approach was provided by Dara and Loos (1985), relating time to heal to the Williams–Landel–Ferry relation for shift in viscosity with time. Determination of an adequate degree of contact can be made using assessment of part quality at different degrees of contact; determination of time heat application is required. It has been found that autohesion times are short even for relatively fast processes such as nonisothermal fusion bonding of thermoplastic sheet (e.g., Bastien and Gillespie, 1991), so that autohesion is not of primary concern in slower processes such as compression molding (Kardos, 1997). Application of pressure does not have a marked effect on degree of autohesion, however, crystallinity during cure may affect such bonding (Lee and Springer, 1987).

Rate of crystallinity must be determined for generally nonisothermal conditions, since control of cooling rate is a key element in tailoring crystallinity to meet mechanical requirements. The dependence of crystallinity on temperature and cooling rate may be generally stated (per Lee and Springer, 1987) as

$$\frac{dc}{dt} = g\left(\frac{dT}{dt}, T\right) \tag{15}$$

where c = crystallinity in the polymer (wt.%), g = experimentally determined material property, and the temperature distribution in the laminate is found by the conservation of energy as

$$\rho C \frac{\partial}{\partial t} = \frac{\partial}{\partial z}\left(k \frac{\partial T}{\partial z}\right) + m_m \frac{dc}{dt} H_U \tag{16}$$

where z = coordinate normal to the laminate plane, ρ = density, C = specific heat, and k = thermal conductivity of the composite.

The degree of crystallinity may be defined conveniently in analogous fashion to degree of cure (Ozawa, 1971; Lee *et al.*, 1987), as

$$c_{ABS} = \frac{H_T}{H_{ULT}} c_r \tag{17}$$

where c_{ABS} = absolute crystallinity in the polymer (wt.%), H_T = heat at temperature T, H_{ULT} = theoretical ultimate heat of crystallinity, and c_r = relative crystallinity in the polymer (wt.%).

Crystallinity drops with faster cooling rates; these rates have been extensively measured and compared (Corrigan *et al.*, 1989). The crystallinity of practical thermoplastic matrices has been shown to be relatively insensitive to changes in hold times during processing, and except for very thick parts, differences in crystallinity in a laminate is not a major concern, despite much work in characterization of crystallinity over process cycles (Cogswell, 1991).

Several basic models have been proposed to couple these morphological and physical parameters with rheological phenomena, particularly for thermoplastic processing, as described in the following two sections.

2.17.4.1 Reinforcement Compaction: Basic Models

In reinforced materials, compression of the composite does not translate directly to pressure to the resin, since a portion of the load is taken up by the fibers for technologically relevant volume fractions (0.5–0.7). Also, laminae must be sufficiently compacted before increasing resin viscosity prevents adequate flow. The presence of fiber–fiber contacts affords a high degree of elastic behavior to the composite during pressurization. Here we focus on the fundamentals of compaction, with part of the discussion of rheological models for combined flow of fibers and fluid reserved for Section 2.17.2 (for an excellent review of this and other compaction and flow phenomena, see also Hubert and Poursartip, 1998). Two types of behavior in compaction are important:

(i) *Compaction of dry reinforcement to maximum fiber volume fraction.* Volume fraction vs. pressure for the reinforcement phase reveals the nature of the fiber–fiber contacts and uniformity of fiber packing. Maximum packing fractions less than 0.785 reveal poor alignment in fibers (Gutowski and Dillon, 1992).

(ii) *Compaction of composite, with resin flowing simultaneously into voids.* Compaction

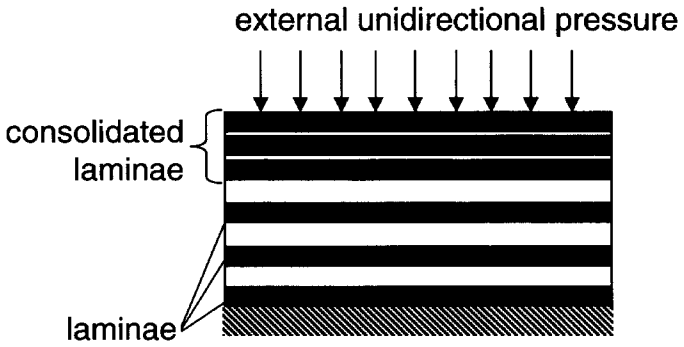

Figure 7 Sequential compaction, as per models by Springer (1982) and Loos and Springer (1983).

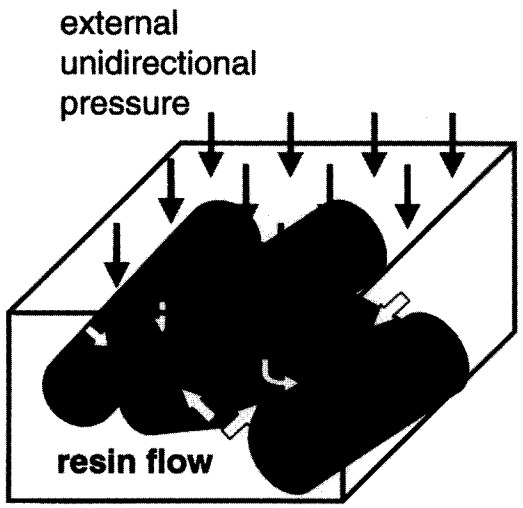

Figure 8 Load-bearing fibers and fiber interconnects in the presence of percolation flow in the assembly due to external pressure.

curves represent the combined effect of resin movement (percolating flow) and fiber compaction. Compaction and permeability are key parameters determining composite response (e.g., Smith and Poursartip, 1993). Effective stress formulations have been derived for composite compaction.

Studies of compaction for the reinforcement phase in liquid molding applications are numerous, and generally address the same phenomena discussed here for laminated materials (e.g. Han *et al.*, 1993). These are generally focused on flow in more irregular architectures, with an eye toward processing with thermosetting resins for SRIM (structural reaction injection molding) and RTM (resin transfer molding) (see Chapter 2.23, this volume). Extensive collection of data on compaction behavior of a large number of textile reinforcements for liquid molding applications in compaction was made by Robitaille and Gauvin (1998). They fitted these data with the semiempirical relation

$$v_f = AP^B \tag{18}$$

where v_f = volume fraction, $A = v_f$ for a pressure of 1 MPa, and B = fitted stiffening index with

$$\frac{P}{P_0} = 1 - Ct^{1/D} \tag{19}$$

where P_o = initial compaction pressure, C = pressure decay after 1 s, D = relaxation index, and t = time.

This allowed comparison of a wide variety of materials' response, including effect of lubricant, or resin, volume fraction, number of layers, and pressure. These phenomena have also been widely studied in textiles, soils, and laminated reinforcements.

Work in the second area, coupled compaction/flow modeling, was pioneered by Loos and Springer (1983) and Springer (1982) who proposed a sequential compaction model (SCM) for laminates. Observation of rigid rods surrounded by liquid undergoing compaction motivated the model assumptions. Resin pressure at the surface of the laminate was assumed to be equal to the vacuum pressure in the bagged part. Pressure in the uncompacted portion of the laminate was assumed to be equal to the applied load. Thus, the model assumed that the resin alone bore the applied pressure, with the resin pressure gradient driving resin flow as layers were forced sequentially into contact via external pressure from one direction (Figure 7).

Later, models wherein resin was assumed to "squeeze" (percolate) through the fibers, producing viscous/elastic load sharing, were developed (derived separately by Davé *et al.*, 1987 and Gutowski *et al.*, 1987). A general case is shown in Figure 8, wherein contacting fibers deform, and resin is simultaneously squeezed throughout the reinforcement during compaction. These squeezed sponge models (SSM) thus

flow around fibers / fiber bundles

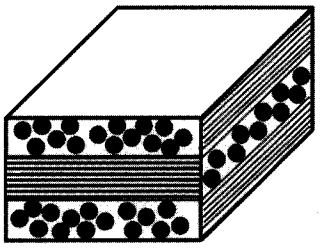

flow / deformation of
an anisotropic continuum

$\{\varepsilon\} = [B]\{\sigma\}$

Figure 9 Two extreme scales of flow modeling in laminated materials.

have the feature that the applied pressure was shared by fibers and resin, and so relate fiber compaction and fiber bed permeability. The apparent inconsistency between the two models was resolved by Hubert and Poursartip (1998) who showed the SCM to be, broadly, a special case of the SSM, by assuming that the fiber layers in the compacted region of the SCM interacted, using a pressure distribution argument. Each SCM and SSM has been implemented with success (for Springer–Loos SCM, see, e.g., numerical/experimental process control work of Ciriscioli *et al.*, 1992; for Davé–Gutowski SSM, see, e.g., numerical implementation by Tredoux and Van der Westhuizen, 1995). For their SSM, Gutowski *et al.* (1987a, 1997b) defined an effective compaction stress as a function of volume fraction

$$\bar{\sigma}(V_f) = \frac{3\pi E_f}{\beta^4} \frac{1 - \sqrt{\frac{V_f}{V_{fo}}}}{\sqrt{\frac{V_a}{V_f} - 1}} \tag{20}$$

where E_f = fiber flexural modulus, β = fiber waviness ratio, V_{fo} = initial volume fraction, and V_a = maximum achievable volume fraction based on beam-bending in the fibers in response to load; this expression had earlier been verified for lubricated systems of graphite fibers in viscous oils. Gutowski and Dillon (1992) reviewed the literature on lubricated carbon fiber bundles and compared their deformation to a 3-D theory by Cai and Gutowski (1992). They were able to collapse a wide range of data using the concept of a bundle "state." This and similar solutions represent models for the cumulative effects of resin flow and reinforcement deformation in 1-D, using simplified assumptions. To model anisotropic flow, greater understanding of the underlying fluid mechanics is involved.

2.17.5 FIBER AND RESIN FLOW, 1-D→3-D

Simplification of modeling the fluid mechanics of resin flowing through the interstices, and between layers, of fiber beds is necessitated by the present impracticality of numerical solution of the full Navier–Stokes equations in a stochastically arranged array of inclusions in the path of the flow front. Thus, modeling is possible at the two extremes shown in Figure 9: at the smallest scale, modeling flow between fibers/fiber bundles, and at the largest scale, treating the laminate as an anisotropic continuum. Selection of modeling scale depends on materials properties and processing type. Four underlying flow mechanisms have been identified by Cogswell (1987) in characterizing flow in thermoplastic materials, though a subset of these also characterizes the major thermosetting flow mechanisms for slow processes. They are (Figure 10): (i) percolation flow, or flow through packed beds; (ii) transverse fiber flow, or "squeezing flow," wherein fluid is forced through the layers via external compression; (iii) intraply shearing between individual, aligned fibers; and (iv) interply slip-cooperative flow, between layers of different (fiber) orientations. These mechanisms stem from consideration of the laminate as a combination of inextensible fibers surrounded by a viscous liquid. Corrections are possible for fiber elasticity, as outlined in the last section.

The first type of flow, percolation in porous media, was described originally by Darcy

Table 2 Commonly implemented creeping flow models with attendant "permeability" k in each case.

	Velocity equation	*Permeability constant*
Darcy flow	$v = \frac{-K}{\mu} \cdot \frac{dP}{dx}$	**K**
Plane Poiseuille flow	$v_{ave} = -\frac{(b^2/3)}{\mu} \cdot \frac{dP}{dx}$	$b^2/3$
Circular Poiseuille flow	$v_{ave} = -\frac{(d^2/32)}{\mu} \cdot \frac{dP}{dx}$	$d^2/32$
Channel with varying thickness	$v_{ave} = \frac{-\left(\frac{4}{3}\frac{a_1^2 a_0^2}{(a_0+a_1)^2}\right)}{\mu} \cdot \frac{dP}{dx}$	$\frac{4}{3}\frac{a_1^2 a_0^2}{(a_0+a_1)^2}$

Source: Senoguz *et al.*, (2000).

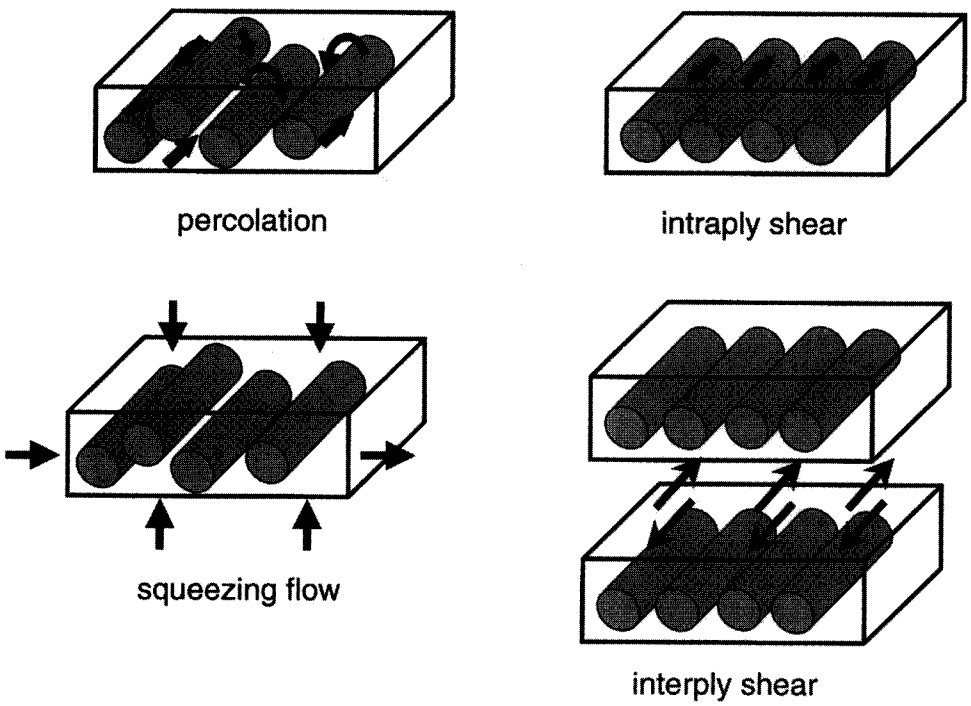

Figure 10 Four types of flow (thermoplastics) as defined by Cogswell (1987).

(1856), who developed the constitutive description by observing water flow through beds of sand. Application to composite processes, from laminates to molded materials, is widespread. The percolation flow is generally applied to thermosetting resins in autoclave (laminate) or liquid molding processes. Though it can be modified to account for differences in axial and transverse flow, i.e., anisotropy in the reinforcement phases (resulting in an anisotropic permeability tensor, described presently), it cannot easily account for mesoscale phenomena as classified by Cogswell (1987). These phenomena are primarily due to shear of layers,

and are key mechanisms in thermoplastic processing because of the higher overall process viscosities. Furthermore, use of thermoforming techniques (e.g., Cogswell, 1991; O'Bradaigh and Mallon, 1989) produces shear between layers, as deformation of thermoplastic sheets onto high curvature parts results in strain gradients in the layers. For these processes, interply slip and shear become very important, and a large body of work exists to model these phenomena. Most composite processes entail a degree of percolation flow, however, as resin must permeate all layers to form well-consolidated laminates, and resin-rich layers are undesirable.

The Darcy model states that pressure gradient is proportional to flow velocity, scaled by the ratio of solid phase permeability to fluid viscosity, as

$$\bar{v} = \frac{-K}{\mu}\nabla P \tag{21}$$

where $\bar{v}$ = average velocity of fluid, μ = viscosity of fluid, K = permeability of porous medium, and ∇P = pressure gradient.

The proportionality of velocity and pressure gradient, in fact, is central to modeling classic creeping flows, wherein the scaling parameter, "permeability," may be derived as in Table 2. This relationship has been commonly used to model polymeric flow in composite materials in the last 20 years (see, e.g., review by Coulter and Guceri, 1988). Though a large fraction of the effort has been devoted to liquid molding of thermosets rather than autoclave processing, the same mathematical formulations are commonly used.

Williams *et al.* (1974) considered the flow of several fluids through aligned reinforcements, both dry and presaturated with liquid. They obtained higher permeabilities for saturated than for unsaturated reinforcement, as did Martin and Son (1986). Many authors since the late 1980s have studied the permeability of fibrous preforms for liquid molding, including Parnas *et al.* (1997), Adams and Rebenfeld (1991a, 1991b), Gauvin *et al.* (1996), Chan *et al.* (1993), Gebart (1992), Rudd *et al.* (1996), Skartsis *et al.* (1992a, 1992b, 1992c), Young and Wu (1995) and Mogavero and Advani (1997). More recent work has focused on complex geometries. Rudd *et al.* (1996) established "permeability maps" for complex geometries. Smith *et al.* (1997) related permeabilities of sheared fabrics to ply angle. Lai and Young (1997) related similar experimental data to a geometry-based flow model. Various authors have suggested that capillarity plays a role in these processes; the effect in real liquid molding processes has been computed to be small (Dungan *et al.*, 2000; Senoguz *et al.*, 2000). Darcy's law implementations uniformly require determination of permeability (in the form of a tensor in anisotropic preforms, where up to three scalar permeabilities are required in the plane case). In these complex geometries, a common approach to handle reinforcement deformation has been to alter the permeabilities obtained for the reinforcement in the undeformed configuration, generally via tensor transformation.

The Darcy approach is, without exception, modified in application to real processing to account for flow "tortuosity" or circuitousness of the path that must be traversed to penetrate the material, the shape of the particles, material anisotropy, and the overall volume fraction. Various modifications to Darcy's law have been proposed in the polymer processing arena and in other areas of fluid–structure interaction; for example, Kozeny (1927) treated a permeated porous medium as a bundle of capillary tubes and obtained a relationship to adapt Darcy's law to include capillarity effects with an empirical relation; Blake (1922) derived a similar expression. Carman (1937) modified Kozeny's work by defining S, the specific surface with respect to a unit volume of solid, instead of a unit volume of porous medium. The "Kozeny–Carmen relationship" arose through these sequential contributions. Carman (1937) experimentally determined a range of "Kozeny constants" for a variety of packing schemes and geometries of reinforcements. This constant is determined empirically from

$$K = \frac{r_f^2}{4k}\frac{(1 - V_f)^3}{V_f^2} \tag{22}$$

wherein k is a constant based on the geometric form of the fibrous bed, and r_f is the fiber diameter. Gutowski *et al.* (1987b) suggested a modification of Equation (22) as

$$K_2 = \frac{r_f^2}{4k'}\frac{\left(\sqrt{\frac{V_a}{V_f}}\right)^3}{\left(\frac{V_a}{V_f} + 1\right)} \tag{23}$$

so that the transverse permeability (K_2) would be zero in the case of maximum volume fraction, since tangency of the cylindrical fibers would effectively block resin flow transverse to the assembly.

Use of the percolation model can be problematic under two commonly occurring conditions in laminate processing (e.g., Astrom *et al.*, 1992; Skartsis *et al.*, 1992c):

(i) The fluid is non-Newtonian.

(ii) Significant anisotropy in the reinforcement phase is present.

Determination of the Deborah number (De) allows assessment of viscoelastic effects; higher values corresponded to greater viscoelastic effects (Astrom *et al.*, 1992; Chmielewski *et al.*, 1990). Anisotropy in the form of aligned fibers can be handled to some extent by corrections to Darcy's law. Rewriting Equation (21) to account for anisotropic permeabilities, one can derive a permeability tensor. Assuming transverse isotropy and scaling permeabilities by the Kozeny–Carmen relation, Astrom *et al.*, (1992) derived

$$S = \frac{r_f^2}{4k}\frac{(1-V_f)^3}{V_f^2}\begin{bmatrix} \frac{1}{(K_o K_1^2)_1} & 0 & 0 \\ 0 & \frac{1}{(K_o K_1^2)_2} & 0 \\ 0 & 0 & \frac{1}{(K_o K_1^2)_3} \end{bmatrix} \quad (24)$$

in which an expression for transverse permeability such as Equation (23) might be substituted for Kozeny–Carmen correction for the transverse terms.

Percolation flow was assumed in the classic compaction work of the SCM model by Springer (1982), Loos and Springer 1983), and the SSM-type models, by Davé *et al.* (1987) and Gutowski *et al.* (1987a, 1987b). In a detailed comparison of the two models by Hubert and Poursartip (1998), the resin velocities in both models for the compacting laminate were compared. In the SCM, they calculated the uniform resin velocities in the compacted zone following the original author's use of a Darcy relationship, i.e., proportionality of resin velocity and pressure gradient. Resin velocity in the uncompacted zone was assumed to be zero, as in the original model. An expression for pressure distribution in the compacted zone due to the fibers was derived for this model via static equilibrium. Resin-fiber load sharing was assumed, with linear resin pressure distribution producing constant resin velocity in that zone, as given in the original work. In the SSM, resin velocity profiles were calculated in the entire laminate, using the original authors' fiber bed compaction model to determine pressure gradients. Using numerical sensitivity studies of a test case (AS4/3501-6 resin), they verified the importance of the fiber bed compaction curve and the material permeability in modeling compaction/consolidation. Permeability was found to affect compaction time strongly, but not to alter compaction behavior. The time to compaction, probably the most important manufacturing parameter, was fastest when the compaction curve was nonlinearly stiffening.

Flow behavior in thermoplastics particularly must be analyzed at higher scales than for percolation or squeezing phenomena alone, due to higher process viscosities and thus greater cohesion in laminae than in thermosetting composites. These models are geared toward understanding of shear flow, since fibers and resin are assumed to move together and thus are treated as a continuum at some scale (as in Figures 9 and 10). The remaining discussion divides description of work in the intraply and interply mechanisms, and laminate scale modeling.

Transverse flow was discussed by Barnes and Cogswell (1989) who described fibers slipping past one another due to compression, in the plane of the part, but perpendicular to fiber axes. Due to fiber twisting, this process was described as self-limiting. Like autohesion at the molecular scale, and percolation flow at the microscale, this phenomenon is a healing process which contributes to part uniformity.

Intraply shear results from fibers slipping axially past one another in a lamina. The first constitutive description of this phenomenon was provided by Rogers (1989a, 1989b) who wrote the material stress tensor as comprised of a sum of terms for composite viscosity matrix and reaction stress due to kinematic constraints, as

$$\sigma_{ij} = D_{ijkl}d_{kl} + r_{ij} \quad (25)$$

where σ = stress, D = composite viscosity matrix, d = deformation rate, and r = reaction stress due to kinematic constraints.

Per this model, the key parameters to be determined experimentally are Δ_L and Δ_T, the composite longitudinal and transverse shears, respectively, which have been measured by a number of workers; significant scatter in reported values exists (e.g., Wheeler and Jones, 1991).

Interply shear is largely an effect seen in shape forming of thermoplastics rather than laminate processing (e.g., Jones and Oakley, 1990). With an assumption of viscoelastic response of the laminae (elastic plies separated by viscous layers), they deduced that intraply shear produced non-Newtonian behavior in the laminate.

Modeling laminates at the scale of an anisotropic continuum has also been performed, with constitutive response described for the matrix as both Newtonian and power-law by Pipes *et al.* (1991a, 1991b, 1992a, 1992b) and Beaussart *et al.* (1993). The constitutive rule,

$$\begin{bmatrix} \dot{\varepsilon}_1 \\ \dot{\varepsilon}_2 \\ \dot{\varepsilon}_3 \\ \dot{\varepsilon}_4 \\ \dot{\varepsilon}_5 \\ \dot{\varepsilon}_6 \end{bmatrix} = \begin{bmatrix} \beta_{11} & -\beta_{11}/2 & -\beta_{11}/2 & 0 & 0 & 0 \\ & \beta_{22} & (\beta_{11}-2\beta_{22})/2 & 0 & 0 & 0 \\ & & \beta_{22} & 0 & 0 & 0 \\ & & & 4\beta_{22}-\beta_{11} & 0 & 0 \\ & & & & \beta_{66} & 0 \\ & & & & & \beta_{66} \end{bmatrix} \begin{bmatrix} \sigma_1 \\ \sigma_2 \\ \sigma_3 \\ \sigma_4 \\ \sigma_5 \\ \sigma_6 \end{bmatrix} \quad (26)$$

where axial elongation viscosity, $\eta_{11} = \beta_{11}^{-1}$ axial shear viscosity, $\eta_{12} = \eta_{66}^{-1}$ transverse elongation viscosity $\eta_{22} = \beta_{22}^{-1}$, and transverse shear viscosity $\eta_{23} = (4\beta_{22} - \beta_{11})^{-1} = (4\eta_{22}^{-1} - \eta_{11}^{-1})^{-1}$ treats the composite as a viscous material, with the fibers' contribution arising from a micromechanical, shear-lag type assumption of matrix shear on inextensible fibers.

Combined analysis of these modes is of greatest importance in the case of shape forming of thermoplastics. For thermosets, and flat panels of thermosets and thermoplastics, percolation flows generally allow assignation of key process variables.

2.17.6 SUMMARY AND FUTURE DIRECTIONS

As computing speeds continually increase, and demands for more complex geometries in composites grows beyond the lower curvature or flat parts of interest to the aerospace industry, it is likely that greater microscale heat transfer, fluid mechanics, and reinforcement deformation mechanics will be undertaken numerically. Investigations by polymer scientists into the kinetics of thermoset reactions will undoubtedly be implemented simultaneously with these.

At the present time, state of the art in flow simulations involves consideration of flow at the scale of the composite, with flow around fibers and tows not explicitly considered other than in an average sense in practical manufacturing simulations. Related flow phenomena have been investigated for thermoplastics, due to the greater importance of shear and the availability of shape forming through thermoforming of these materials.

In resin kinetics for thermosetting materials, work continues on investigations of the contributions of individual reactions in epoxy systems. The successful implementation of these models will draw on existing, available heat transfer simulations which currently can predict temperature distributions in laminates with high accuracy. Molecular motion in thermoplastics has been investigated (autohesion), with the general finding that for slower processes (autoclave processing and compression molding) the required diffusion times are modest to assure good interlaminar distribution of the matrix.

In fiber bed compaction, compressibility of reinforcement will be of growing interest in the coming years as more complex geometric shapes for composites are realized. The interplay between fiber bed compaction and resin flow has been studied in some detail, and at present, semiempirical models have been implemented in numerical codes which satisfactorily predict combined compaction/flow behavior.

Overall, work on impregnation and consolidation in thermoplastic and thermoset materials has overlapped. With greater opportunity for molecular and microscale modeling available in the coming years, it is likely that techniques will diverge somewhat. At the present time, however, suitable models for these phenomena exist, and have been shown to be realistic in a broad range of manufacturing settings.

ACKNOWLEDGMENTS

The author gratefully acknowledges the kind assistance of L. Berhan, B. Crawford, F. Dungan, J. Ottaviani, and C. W. Wang in helping to collect materials for this work.

2.17.7 REFERENCES

K. L. Adams and L. Rebenfeld, *Polym. Compos.*, 1991a, **12**, 179–185.
K. L. Adams and L. Rebenfeld, *Polym. Compos.*, 1991b, **12**, 186–190.
B. T. Astrom, R. B. Pipes and S. G. Advani, *J. Compos. Mater.*, 1992, **26**, 1351–1373.
J. A. Barnes and F. N. Cogswell, *Composites*, 1989, **20**, 38–42.
L. J. Bastien and J. W. Gillespie, *Polym. Engg. Sci.*, 1991, **31**, 1720–1730.
A. J. Beaussart, J. W. S. Hearle and R. B. Pipes, *Compos. Sci. Technol.*, 1993, **49**, 335–339.
F. C. Blake, *Trans. Am. Inst. Chem. Eng.*, 1922, **14**, 415–421.
Z. Cai and T. G. Gutowski, *J. Compos. Mater.*, 1992, **26**, 1207–1237.
P. C. Carman, *Trans. Inst. Chem. Engrs.*, 1937, **15**, 150–156.
B. Chabert, G. Lachenal and C. V.-Tung, *Macromol. Symp.*, 1995, **94**, 145–158.
A. W. Chan, D. E. Larive and R. J. Morgan, *J. Compos. Mater.*, 1993, **27**, 996–1008.

C. Chmielewski, C. A. Petty and K. Jayaraman, *J. Non-Newtonian Fluid Mech.*, 1990, **35**, 309–325.
P. R. Ciriscioli, G. S. Springer and W. I. Lee, *SAMPE J.*, 1989, **25**, 35–42.
P. R. Ciriscioli and G. S. Springer, *J. Compos. Mater.*, 1992, **26**, 90–102.
P. R. Ciriscioli, Q. Wang and G. S. Springer, *J. Compos. Mater.*, 1991, **25**, 1542–1587.
F. N. Cogswell, *Int. Polym. Processing*, 1987, **14**, 157–165.
F. N. Cogswell, *Compos. Manuf.*, 1991, **2**, 208–216.
F. N. Cogswell, 'Thermoplastic Aromatic Polymer Composites', Butterworth-Heinemann Ltd., Oxford, UK, 1992.
E. Corrigan, D. C. Leach and T. McDaniels, in 'Proceedings of the 10th International European SAMPE Conference', Materials Science Monographs, Elsevier, Oxford, UK, 1989, pp. 2057–2064.
J. P. Coulter and S. I. Guceri, in 'Proceedings of Manufacturing International 88', Atlanta, GA, American Society of Mechanical Engineers, New York, 1988, pp. 79–86.
P. H. Dara and A.C. Loos, 1985, Report CCMS-85-10, BPI-E-85-21, Virginia Polytechnic Institute and State University, Blacksburg, VA.
H. Darcy, 'Les fontaines publiques de la ville de Dijon', Valmont, Paris, 1856.
R. Davé, J. L. Kardos and M. P. Dudukovic, *Polym. Compos.*, 1987, **8**, 29–38.
C. J. de Bakker, N. A. St John and G. A. George, *Polymer*, 1993, **34**, 716–725.
F. D. Dungan, M. T. Senoguz and A. M. Sastry, *J. Compos. Mater.*, 2000, manuscript submitted.
R. Gauvin, F. Trochu, Y. Lemenn and L. Diallo, *Polym. Compos.*, 1996, **17**, 34–42.
B. R. Gebart, *J. Compos. Mater.*, 1992, **26**, 1100–1133.
P. G. de Gennes, *J. Chem. Phys.*, 1971, **55**, 572–579.
T. G. Gutowski, Z. Cai, S. Bauer, D. Boucher, J. Kingery and S. Wineman, *J. Compos. Mater.*, 1987a, **21**, 650–669.
T. G. Gutowski and G. Dillon, *J. Compos. Mater.*, 1992, **26**, 2330–2347.
T. G. Gutowski, T. Morigaki and Z. Cai, *J. Compos. Mater.*, 1987b, **21**, 172–188.
K. Han, L. Trevino, L. J. Lee and M. Liou, *Polym. Compos.*, 1993, **14**, 144–160.
J. C. Halpin, J. L. Kardos and M. P. Dudukovic, *Pure & Appl Chem.*, 1983, **55**, 893–906.
P. Hubert and A. Poursartip, *J. Reinf. Plast. Compos.*, 1998, **17**, 286–318.
R. S. Jones and D. Oakley, *Composites*, 1990, **21**, 415–418.
J. L. Kardos, in 'Advanced Composites Manufacturing', ed. T. G. Gutowski, Wiley, New York, 1997.
J. Kozeny, *Sitzungsber. Akad. Wiss. Wien*, 1927, **136**, 271–301.
G. Lachenal, N. Poisson and J. Sautereau, *Macromol. Symp.*, 1997, **119**, 129–136.
C.-L. Lai and W.-B. Young, *Polym. Compos.*, 1997, **18**, 642–648.
W. I. Lee, A. C. Loos and G. S. Springer, *J. Compos. Mater.*, 1982, **16**, 510–520.
W. I. Lee and G. S. Springer, *J. Compos. Mater.*, 1987, **21**, 1017–1055.
W. I. Lee, M. F. Talbott, G. S. Springer and A. Berglund, *J. Reinf Plast Compos.*, 1987, **6**, 2–12.
A. C. Loos and G. S. Springer, *J. Compos. Mater.*, 1983, **17**, 135–169.
G. Q. Martin and J. S. Son, in 'Proceedings of the 2nd Conference on Advanced Composites', Dearborn, MI, ASM International, Metals Park, OH, 1986, pp. 149–157.
J. Mogavero and S. G. Advani, *Polym. Compos.*, 1997, **18**, 649–655.
R. S. Parnas, K. M. Flynn and M. E. Dal-Favero, *Polym. Compos.*, 1997, **18**, 623–633.
C. M. O'Bradaigh and P. J. Mallon, *Compos. Sci. Technol.*, 1989, **35**, 235–255.
T. Ozawa, *Polymer*, 1971, **12**, 150–158.
R. B. Pipes, *J. Compos. Mater.*, 1992, **26**, 1536–1552.
R. B. Pipes, A. J. Beaussart, J. T. Tzeng and R. K. Okine, *J. Compos. Mater.*, 1992, **26**, 1088–1099.
R. B. Pipes, J. W. S. Hearle, A. J. Beaussart and R. K. Okine, *J. Compos. Mater.*, 1991a, **25**, 1379–1390.
R. B. Pipes, J. W. S. Hearle, A. J. Beaussart, A. M. Sastry and R. K. Okine, *J. Compos. Mater.*, 1991b, **25**, 1204–1217.
R. B. Prime, *Polym. Eng Sci.*, 1973, **13**, 365–371.
F. Robitaille and R. Gauvin, *Polym. Compos.*, 1998, **19**, 198–216.
F. Rodriguez, 'Principles of Polymer Systems', Taylor & Francis, Washington, DC, 1996.
T. G. Rogers, *J. Eng Math.*, 1989a, **23**, 81–89.
T. G. Rogers, *Composites*, 1989b, **20**, 21–27.
C. D. Rudd, A. C. Long, P. McGeehin and P. Smith, *Polym. Compos.*, 1996, **17**, 52–59.
M. T. Senoguz, F. D. Dungan, A. M. Sastry and J. T. Klamo, *J. Compos. Mater.*, 2000, manuscript submitted.
L. Skartsis, J. L. Kardos and B. Khomami, *Polym. Eng. Sci.*, 1992a, **32**, 221–230.
L. Skartsis, B. Khomami and J. L. Kardos, *Polym. Eng. Sci.*, 1992b, **32**, 231–239.
L. Skartsis, B. Khomami and J. L. Kardos, *J. Rheol*, 1992c, **36**, 589–620.
G. D. Smith and A. Poursartip, *J. Compos. Mater.*, 1993, **27**, 1695–1711.
P. Smith, C. D. Rudd and A. C. Long, *Compos. Sci.*, 1997, **57**, 52–59.
S. Sourour and M. R. Kamal, *Thermochim Acta*, 1976, **14**, 41–59.
G. S. Springer, *J. Compos. Mater.*, 1982, **16**, 400–410.
R. P. Theriault, T. A. Osswald and J. M. Castro, *Polym. Compos.*, 1999, **20**, 628–633.
L. Tredoux and J. Van der Westhuizen, *Compos. Manuf.*, 1995, **6**, 85–92.
A. B. Wheeler and R. S. Jones, *Comp. Manuf.*, 1991, **2**, 192–196.
J. G. Williams, C. E. Morris and B. C. Ennis, *Polym. Eng. Sci.*, 1974, **14**, 413–419.
R. P. Wool, *J. Rheol.*, 1982, **26**, 575–575.
R. P. Wool and K. M. O'Connor, *J. Appl. Phys.*, 1981, **52**, 5953–5963.
W.-B. Young and S. F. Wu, *J. Reinf. Plas. Compos.*, 1995, **14**, 1108–1120.